JOC Article
pubs.acs.org/joc

Multiple Decomposition Pathways for the Oxenium Ion Precursor *O*-(4-(4′-Methylphenyl)phenyl)-*N*-methanesulfonylhydroxylamine

Yue-Ting Wang and Michael Novak*

Department of Chemistry and Biochemistry, Miami University, Oxford, Ohio 45056

novakm@muohio.edu

Received July 2, 2009

Downloaded by EXETER UNIV on October 17, 2009 | http://pubs.acs.org
Publication Date (Web): September 23, 2009 | doi: 10.1021/jo9014062

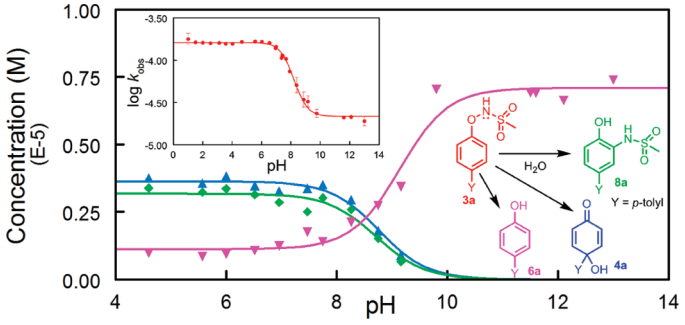

Although *O*-arylhydroxylamine derivatives have been claimed to be sources of oxenium ions in a large number of studies, it is not clear that the products of these reactions are due to oxenium ions. Previously, we had shown through azide trapping studies that the quinol ester **2a** and the title compound **3a** generate the oxenium ion **1a**. The ester **2a** exclusively generates **1a** in water and is also a photoprecursor of **1a** in water. This is not true of **3a**. The oxenium ion pathway accounts for a significant fraction of the reaction of **3a** under neutral and acidic pH conditions, but there are three other pathways that account for hydrolysis of **3a**. Both **3a** and its conjugate base **3a**$^-$ are present in aqueous solution under mild pH conditions. In addition to the oxenium ion product **4a**, two other significant products are generated: the phenol **6a** and the rearrangement product **8a**. Both **4a** and **8a** are generated exclusively from **3a**, whereas **6a** is generated from both **3a** and **3a**$^-$. Azide trapping studies show that **6a** and **8a** are not generated from the oxenium ion. The phenol **6a** is generated by two paths, one involving an apparent radical intermediate **7a** and the other through a stepwise α-elimination pathway through **3a**$^-$. The rearrangement product **8a** is generated either through a concerted rearrangement or via an ion-pair rearrangement. Photolysis of **3a** does not generate **1a**. The only products of photolysis of **3a** in water are **6a** (major) and **8a** (minor). The weak O−N bond of **3a** is susceptible to homolysis under photolysis conditions, and the radical **7a** is observed after laser flash photolysis of **3a**. The cation **1a** that is observed during laser flash photolysis experiments on **2a** cannot be detected during similar experiments on **3a**. These results suggest that the previous attribution of oxenium ions as the source of the decomposition products of other *O*-arylhydroxylamine derivatives in aromatic solvents via thermolysis or acid-catalyzed decomposition may not be correct.

Introduction

Early mechanistic investigations into the potential generation of aryloxenium ions, **1**, via heterolytic bond dissociation processes concentrated on the utilization of *O*-arylhydroxylamine derivatives as precursors to these ions in aromatic solvents via thermolysis or acid-catalyzed decomposition.[1−10] Interpretation of results was difficult because reaction products generated from similar precursors were significantly different from each other.[1−4,6−9] Furthermore, the isolated products were considerably different from those

(1) Abramovitch, R. A.; Inbasekaran, M.; Kato, S. *J. Am. Chem. Soc.* **1973**, *95*, 5428–5430.
(2) Abramovitch, R .A.; Alvernhe, G.; Inbasekaran, M. N. *Tetrahedron Lett.* **1977**, 1113–1116.
(3) Abramovitch, R. A.; Inbasekaran, M. N. *J. Chem. Soc., Chem. Commun.* **1978**, 149–150.
(4) Abramovitch, R. A.; Alvernhe, G.; Bartnik, R.; Dassanayake, N. L.; Inbasekaran, M. N.; Kato, S. *J. Am. Chem. Soc.* **1981**, *103*, 4558–4565.

DOI: 10.1021/jo9014062 Published on Web 09/23/2009
© 2009 American Chemical Society

SCHEME 1. Products Attributed to Aryloxenium Ions Generated under Different Reaction Conditions

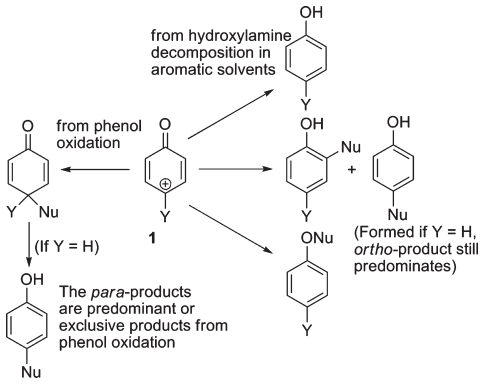

obtained via oxidation reactions of phenols that were also thought to generate oxenium ions.[11−16] Specifically, the *O*-arylhydroxylamine derivatives led to predominant attack by nucleophiles at the *ortho* position of the purported cations, whereas the apparent cations generated by phenol oxidation led to predominant nucleophilic attack at the *para* position (Scheme 1). The decomposition of the *O*-arylhydroxylamine derivatives in aromatic solvents also often led to products of apparent nucleophilic attack on the oxygen of the alleged cation and to phenols that were thought to arise from H-abstraction by a triplet oxenium ion.[1−4,9] The triplet pathway did not appear to be viable because low level ab initio calculations (MP2/3-21G//STO-3G) suggested that the singlet is the ground state for unsubstituted (Y = H) **1** by ca. 30 kcal/mol.[5] It has been argued that the products of apparent nucleophilic attack on oxygen of the cation are due, instead, to a concerted S_N2-like process, but no convincing experimental evidence for this pathway has been presented.[9]

More recently we have utilized the 4-(*p*-tolyl) quinol ester **2a** and *O*-(4-(4′-methylphenyl)phenyl)-*N*-methanesulfonylhydroxylamine **3a** to generate the oxenium ion **1a** in an aqueous environment (Scheme 2).[17] Under hydrolysis conditions from pH 1 to 8, **2a** generates **4a** as the only detectable product. In the presence of N_3^- **4a** is replaced by the azide-adduct **5a** with no increase in the rate constant for decomposition of **2a**.[17] Phenol **6a** was not detected under these

SCHEME 2. Previously Demonstrated Reaction Pathways for 2a and 3a[17,22,23]

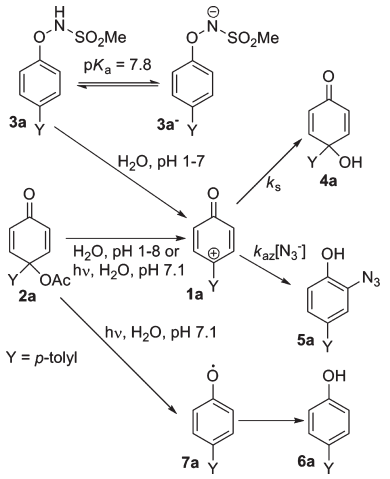

conditions.[17] This result is consistent with recent calculations suggesting that the triplet oxenium ion is ca. 20 kcal/mol less stable than the singlet species.[18,19] Under hydrolysis conditions all available evidence is consistent with the conclusion that **2a** leads exclusively to the singlet ion **1a**. Similar conclusions were reached for the 4-phenyl quinol ester **2b** and the 4-(*p*-bromophenyl) quinol ester **2c**.[17,20,21] Under laser flash photolysis conditions both **1a** and the aryloxy radical **7a** are generated from photolysis of **2a** in aqueous solution.[22,23] Since their UV spectra do not overlap significantly, these species can be separately characterized. The oxenium ion (λ_{max} 460 nm) decays in a first-order manner, reacts with N_3^- at a diffusion controlled rate, and is insensitive to O_2, whereas the radical (λ_{max} 360 nm) undergoes reversible dimerization resulting in biphasic decomposition kinetics, is insensitive to N_3^-, is somewhat sensitive to O_2, and does yield **6a** as a major reaction product.[22,23] The hydroxylamine derivative **3a** was shown, in part, to generate the oxenium ion **1a** in aqueous solution through heterolytic O−N bond dissociation because the same hydrolysis product **4a** was observed, and that product was trapped out by N_3^- to yield **5a** with a selectivity ratio, k_{az}/k_s, 1.2×10^3 M^{-1} that was experimentally equivalent to that observed for **2a** (Scheme 2).[17]

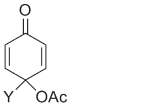

2b Y = phenyl
2c Y = *p*-Brphenyl

The hydrolysis chemistry of **2a** is particularly simple since it generates only **1a** at all pH examined.[17] Although azide

Downloaded by EXETER UNIV on October 17, 2009 | http://pubs.acs.org
Publication Date (Web): September 23, 2009 | doi: 10.1021/jo9014062

(5) Li, Y.; Abramovitch, R. A.; Houk, K. N. *J. Org. Chem.* **1989**, *54*, 2911–2914.
(6) Endo, Y.; Shudo, K.; Okamoto, T. *J. Am. Chem. Soc.* **1977**, *99*, 7721–7723.
(7) Shudo, K.; Orihara, Y.; Ohta, T.; Okamoto, T. *J. Am. Chem. Soc.* **1981**, *103*, 943–944.
(8) Endo, Y.; Shudo, K.; Okamoto, T. *J. Am. Chem. Soc.* **1982**, *104*, 6393–6397.
(9) Iijima, H.; Endo, Y.; Shudo, K.; Okamoto, T. *Tetrahedron* **1984**, *40*, 4981–4985.
(10) Uto, K.; Miyazawa, E.; Ito, K.; Sakamoto, T.; Kikugawa, Y. *Heterocycles* **1998**, *48*, 2593–2600.
(11) Swenton, J. S.; Carpenter, K.; Chen, Y.; Kerns, M. L.; Morrow, G. W. *J. Org. Chem.* **1993**, *58*, 3308–3316.
(12) Kerns, M. L.; Conroy, S. M.; Swenton, J. S. *Tetrahedron Lett.* **1994**, *35*, 7529–7532.
(13) Swenton, J. S.; Callinan, A.; Chen, Y.; Rohde, J. L.; Kerns, M. L.; Morrow, G. W. *J. Org. Chem.* **1996**, *61*, 1267–1274.
(14) Rieker, A.; Beisswenger, R.; Regier, K. *Tetrahedron* **1991**, *47*, 645–654.
(15) Rieker, A.; Speiser, B.; Straub, H. *DECHEMA Monogr.* **1992**, *125*, 777–782.
(16) Pelter, A.; Ward, R. S. *Tetrahedron* **2001**, *57*, 273–282.
(17) Novak, M.; Poturalski, M. J.; Johnson, W. L.; Jones, M. P.; Wang, Y.-T.; Glover, S. A. *J. Org. Chem.* **2006**, *71*, 3778–3785.
(18) Glover, S. A.; Novak, M. *Can. J. Chem.* **2005**, *83*, 1372–1381.
(19) Wang, Y.-T.; Jin, K. J.; Myers, L. R.; Glover, S. A.; Novak, M. *J. Org. Chem.* **2009**, *74*, 4463–4471.
(20) Novak, M.; Glover, S. A. *J. Am. Chem. Soc.* **2004**, *126*, 7748–7749.
(21) Novak, M.; Glover, S. A. *J. Am. Chem. Soc.* **2005**, *127*, 8090–8097.
(22) Wang, Y.-T.; Wang, J.; Platz, M. S.; Novak, M. *J. Am. Chem. Soc.* **2007**, *129*, 14566–14567.
(23) Wang, Y.-T.; Jin, K. J.; Leopold, S. H.; Wang, J.; Peng, H.-L.; Platz, M. S.; Xue, J.; Phillips, D. L.; Glover, S. A.; Novak, M. *J. Am. Chem. Soc.* **2008**, *130*, 16021–16030.

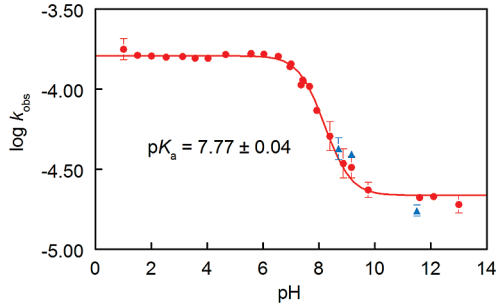

FIGURE 1. pH dependence of the decomposition of **3a** at 30 °C. Red circles correspond to k_{obs} for decomposition of **3a** obtained by UV spectroscopy. Blue triangles correspond to the rate constants obtained by HPLC. Data were fit to eq 1 as described in the text.

trapping clearly shows that **3a** also generates **1a**, there were indications in our earlier study that the chemistry of **3a** is more complicated than that of **2a**. Ionization of **3a** to form its conjugate base **3a**$^-$ near neutral pH was demonstrated by spectrophotometric titration (pK_a = 7.8 ± 0.1). The rate of decomposition of **3a** slowed considerably near its pK_a, but there were indications that its conjugate base was also reactive in aqueous solution.[17] Preliminary results showed that the yield of **4a** decreased at pH > 8, and products other than **4a** were detected by HPLC at all pH examined. Because of the previous ambiguity of interpretation of the results for the decomposition of other *O*-arylhydroxylamine derivatives we decided to examine the chemistry of **3a** in more detail. The results presented herein show that **3a** has three distinct decomposition paths in aqueous solution: a heterolysis to generate the cation **1a**, a rearrangement pathway, and an apparent homolysis to generate **7a**, and ultimately **6a**. The conjugate base **3a**$^-$ has another unique decomposition mechanism involving an α-elimination to form **6a** and a nitrene. Photolysis of **3a** in aqueous solution is not a viable pathway to the oxenium ion, **1a**, but does yield **7a** as a readily detectable transient intermediate.

Results and Discussion

Hydrolysis Reactions. Within the pH range examined previously, the decomposition of **3a** remains pH-independent from pH 1 to 7 and exhibits a decrease in the reaction rate from pH 7 to 9 that appears to be associated with ionization of **3a**.[17] For the current study, additional reaction kinetics were measured at 30 °C in pH 5−8 NaH_2PO_4/Na_2HPO_4 buffers, pH 7−9 TrisH$^+$/Tris buffers, pH 9.8 HCO_3^-/CO_3^{2-} buffer, and pH 11−13 NaOH solutions (5 vol % CH_3CN/H_2O, μ = 0.5 ($NaClO_4$)) by monitoring changes in UV absorbance as a function of time. Because of the low solubility of **3a** in water, all reactions were performed with an initial concentration of **3a** of ca. 1 × 10^{-5} M to prevent precipitation. Rate constants taken at two wavelengths were averaged at each pH to obtain k_{obs}. All k_{obs} for **3a** are provided in Supporting Information. Rate constants measured in 0.01−0.04 M phosphate and Tris buffers are independent of buffer concentration (Supporting Information). Rate constants reported in Supporting Information were taken in 0.02 M buffer and were not extrapolated to 0 M buffer. Kinetic data were also gathered by monitoring changes in HPLC peak area versus time for **3a** and its decomposition products.

TABLE 1. Derived Rate Parameters for Decomposition of 3a[a]

T (°C)	k_o (s^{-1})	k_- (s^{-1})	pK_a
30	(1.62 ± 0.03) × 10^{-4}	(2.17 ± 0.07) × 10^{-5}	7.77 ± 0.04

[a]Determined by a nonlinear least-squares fit of the kinetic data to eq 1.

The pH dependence of the decomposition of **3a** is summarized in Figure 1. The k_{obs} for decomposition of **3a** at pH 1−13 were fit to the rate law of eq 1. The derived rate constants are presented in Table 1.

$$k_{obs} = k_o([H^+]/(K_a+[H^+]))+k_-(K_a/(K_a+[H^+])) \quad (1)$$

The first term of eq 1 corresponds to a pH-independent decomposition of neutral **3a**. The second term of eq 1 corresponds to the uncatalyzed decomposition of its conjugate base **3a**$^-$. The dominant process at pH ≥ 9 is the uncatalyzed decomposition of **3a**$^-$. The rate constant for decomposition of **3a**$^-$, k_-, is ca. 7.5-fold smaller than the rate constant for decomposition of its conjugate acid, k_o. Over the entire range of pH examined the rate of decomposition of **3a** varies by less than an order of magnitude. The kinetic pK_a of **3a**, 7.77 ± 0.04, corresponds to the previously observed spectrophotometric pK_a of 7.8 ± 0.1.[17]

Three major reaction products were detected by HPLC throughout the pH range of the study. These are the previously identified quinol **4a**,[17] the phenol **6a**, and the rearranged product **8a**. At pH ≤ 8, **4a** and **8a** are the major products. At pH ≥ 10, **6a** is the only significant product detected. The time course of the decomposition of **3a** and the formation of these products can be followed by HPLC. Figure 2 shows the kinetics of reactant decay and product formation for reactions carried out in pH 8.7 and 9.2 Tris buffers and in pH 11.5 NaOH solution.

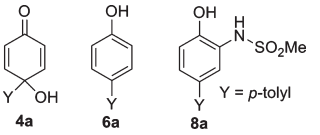

Data for **3a** and the two products **4a** and **6a** fit a standard first-order rate equation at all three pH. A double exponential rate equation was used to fit the data for **8a**. The rate constants obtained for the reaction of **3a** based on HPLC analysis are shown in Table 2. They are comparable to those determined by UV spectroscopy under the same conditions. The rate constants for the disappearance of **3a** from the HPLC experiments are shown with the rate constants obtained from UV experiments in Figure 1.

The yield of the quinol **4a** decreases in Tris buffers at pH > 8.0 compared to less basic buffers, but control experiments and the kinetic results of Figure 2A and B shows that authentic **4a** is stable in Tris buffers. A fast decomposition of authentic **4a** in pH 12.8 NaOH solution was observed. No HPLC peak corresponding to **4a** can be detected within the detection limit after 1 h. Instead, a new peak that has an HPLC retention time similar to **4a** was found. It is likely that **4a** undergoes a base-catalyzed acyloin rearrangement.[24,25]

(24) Uno, H.; Yayama, A.; Suzuki, H. *Chem. Lett.* **1991**, *7*, 1165–1168.
(25) Nishinaga, A.; Itahara, T.; Matsuura, T.; Berger, S.; Henes, G.; Rieker, A. *Chem. Ber.* **1976**, *109*, 1530–1548.

Downloaded by EXETER UNIV on October 17, 2009 | http://pubs.acs.org
Publication Date (Web): September 23, 2009 | doi: 10.1021/jo9014062

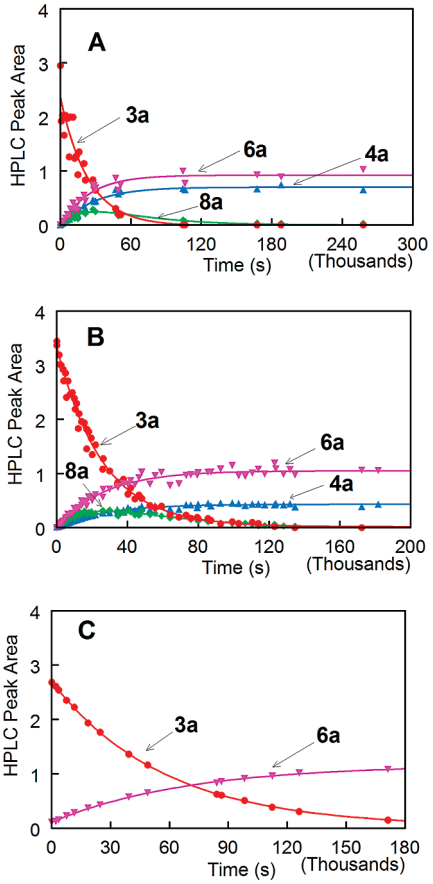

FIGURE 2. HPLC peak area as a function of time for the decomposition of **3a** (red circles) and the formation of **4a** (blue triangles), **6a** (magenta inverted triangles), and **8a** (green diamonds) at 30 °C in pH 8.7 Tris buffer (**A**), pH 9.2 Tris buffer (**B**), and pH 11.5 NaOH solution. In **A** and **B**, peak area data were obtained at 260 nm except for **4a**, which was monitored at 227 nm. In **C** all data were obtained at 269 nm. The data for **3a**, **4a**, and **6a** were fit to a first-order rate equation. The data for **8a** were fit to a double exponential rate equation.

TABLE 2. Rate Constants Obtained by HPLC Analysis of Decomposition of 3a at pH 8.7, 9.2, and 11.5

	$10^5 k_{obs}$ (s^{-1})				
pH	from **3a** at 260/269 nm	from **4a** at 227 nm	from **6a** at 260/269 nm	from **8a** at 260 nm[a]	from **8a** at 260 nm[b]
8.7	4.2 ± 0.7	3.5 ± 0.3	4.1 ± 0.6	3.8 ± 1.9	2.7 ± 1.4
9.2	3.9 ± 0.1	3.7 ± 0.2	3.8 ± 0.2	4.9 ± 1.3	2.7 ± 0.7
11.5	1.7 ± 0.1		1.7 ± 0.1		

[a]Rate constant for the generation of **8a** as **3a** decomposes. [b]Rate constant for the disappearance of **8a**.

Neither **4a** nor its decomposition product were observed during the decomposition of **3a** monitored by HPLC in pH 11.5 NaOH solution (Figure 2C). Neither **4a** nor its decomposition product were detected in NaOH solutions or in HCO_3^-/CO_3^{2-} buffer at the completion of the decomposition of **3a**. The results indicate that **4a** is not generated at pH ≥ 10.

Control experiments confirm that the rearrangement product **8a** is stable in phosphate buffers but does decompose in Tris buffers with rate constants that are somewhat smaller than the rate constants for its formation (Table 2). In more basic NaOH solution, peaks corresponding to **8a** or its decomposition product were not detected. Phenol **6a** is stable under all reaction conditions according to HPLC data.

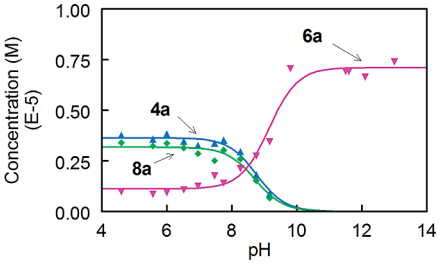

FIGURE 3. Yields of decomposition products of **3a** vs pH. Data for **4a** (blue triangles) and **8a** (green diamonds) were obtained at 227 nm, and data for **6a** (magenta inverted triangles) were obtained at 260 nm. Initial concentration of **3a** is ca. 1×10^{-5} M. Data were fit as described in the text.

The three major products observed by HPLC for the decomposition of **3a** in the absence of strong nonsolvent nucleophiles in aqueous solution were generated in pH and buffer independent yields in the pH range 4−7. These products were isolated from a large scale hydrolysis reaction of **3a** in pH 4.6 acetate buffer at 30 °C. Both **4a** and **6a** were identified by comparison to authentic samples. After isolation and purification from reaction mixtures, the identity of **8a** was confirmed by analysis of spectroscopic data. The individual yields of **4a**, **6a**, and **8a** determined by HPLC quantification after 10 half-lives (ca. 12 h) of the hydrolysis of **3a** are (37.4 ± 1.1)%, (9.1 ± 1.1)%, and (34.3 ± 1.5)%, respectively, in pH 4.6 acetate buffer and (34.5 ± 3.5)%, (12.1 ± 1.1)%, and (28.6 ± 0.5)%, respectively, in pH 7.1 phosphate buffer. In basic solution at pH > 8, the yield of phenol **6a** increases while the yields of **4a** and **8a** decrease with increasing pH. Control experiments confirmed that product yields were not buffer-dependent in Tris buffers. At pH ≥ 10, **6a** becomes the only significant product while **4a** and **8a** are no longer observed. On the basis of HPLC quantification **6a** accounted for (70.6 ± 2.8)% of the decomposition products of **3a** in pH 11.5 NaOH solution. Yields of the three major decomposition products of **3a** in aqueous solution at pH 4−13 obtained by HPLC quantification are summarized in Figure 3. Since **8a** decomposes in basic Tris buffers, its yield under those conditions was determined by extrapolation of its HPLC decay curve to zero time. Data for **4a** and **8a** were fit to eq 2 and eq 3, respectively, in which $[\mathbf{4a}]_o$ or $[\mathbf{8a}]_o$ are the maximum concentrations of **4a** or **8a** formed under acidic conditions. A titration curve (eq 4) was used to fit the concentration vs pH data for **6a**. $[\mathbf{6a}]_o$ and $[\mathbf{6a}]_-$ represent the limiting concentration of **6a** produced from the decomposition of **3a** under acidic and basic conditions, respectively.

$$[\mathbf{4a}] = [\mathbf{4a}]_o([H^+]/(K_a'+[H^+])) \quad (2)$$

$$[\mathbf{5a}] = [\mathbf{5a}]_o([H^+]/(K_a'+[H^+])) \quad (3)$$

$$[\mathbf{6a}] = [\mathbf{6a}]_o([H^+]/(K_a'+[H^+]))+[\mathbf{6a}]_-K_a'/(K_a'+[H^+])) \quad (4)$$

The average apparent pK_a, pK_a', is 8.84 ± 0.19. This pK_a' differs from the thermodynamic pK_a of **3a** (7.77 ± 0.04) since the yield of each product depends on the pK_a of **3a**, and the

Downloaded by EXETER UNIV on October 17, 2009 | http://pubs.acs.org
Publication Date (Web): September 23, 2009 | doi: 10.1021/jo9014062

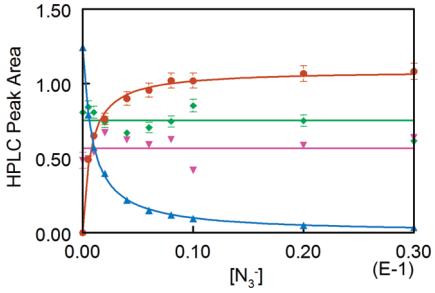

FIGURE 4. Yields of **4a** (blue triangles), **5a** (brown circles), **6a** (magenta inverted triangles), and **8a** (green diamonds) at pH 7.0 in 0.02 M phosphate buffer as a function of $[N_3^-]$. Data were obtained from HPLC analysis at 227 nm (**4a**) and 260 nm (**5a**, **6a**, **8a**). Yields of **4a** and **5a** were fit to the standard "azide clock" equations.[26,27].

TABLE 3. pK_a' **Obtained from Yield vs pH Data for 4a, 6a, and 8a**[a]

	4a	6a	8a	av pK_a'
pK_a'	8.76 ± 0.07	9.15 ± 0.15	8.71 ± 0.09	8.84 ± 0.19

[a]From nonlinear least-squares fits of the yield data to eqs 2-4.

relative magnitudes of k_o and k_-. Since k_o is 7.5-fold larger than k_-, the products generated from **3a** have a kinetic advantage over those from $\mathbf{3a}^-$. The expected relationship between pK_a', pK_a, and k_o/k_- is shown in eq 5. The calculated pK_a' (8.64 ± 0.05), obtained from eq 5 and the kinetic parameters of Table 1, is in good agreement with the average pK_a' derived from product yield versus pH data. These results indicate that **4a** and **8a** are formed exclusively from decomposition of **3a**, whereas **6a** is generated from decomposition of both **3a** and $\mathbf{3a}^-$ via independent pathways.

$$pK_a' = pK_a + \log(k_o/k_-) \quad (5)$$

Previously we showed that the quinol **4a** was efficiently trapped out of the reaction mixtures by N_3^- and replaced by the azide adduct **5a** with no acceleration of the rate of decomposition of **3a**.[17] The selectivity ratio for **3a**, k_{az}/k_s, (see Scheme 2) measured previously was $(1.2 \pm 0.1) \times 10^3$ M^{-1}.[17] This ratio was experimentally indistinguishable from k_{az}/k_s of $(1.0 \pm 0.2) \times 10^3$ M^{-1} measured from azide trapping experiments performed on **2a**.[17] The equivalence of the measured selectivity ratio and of the two reaction products **4a** and **5a** generated from the two different precursors **2a** and **3a** indicated that they both generated the same cation, **1a**.[17] In the current study, the effect of $[N_3^-]$ on the yields of the two other products was examined in pH 7.0 phosphate buffer under reaction conditions identical to those used previously. Results of that study are presented in Figure 4. Data for **4a** and the azide adduct **5a** were fit by least-squares procedures to the standard "azide-clock" equation.[26,27] The observed value of k_{az}/k_s of $(1.3 \pm 0.2) \times 10^3$ M^{-1} is experimentally equivalent to the value previously reported.[17] Although the data are somewhat scattered, the yields of neither **6a** nor **8a** responds significantly to changes in N_3^- concentration under the reaction conditions. This indicates that the pathways leading to **6a** and **8a** do not involve the cationic intermediate **1a** that is trapped by N_3^-.

The dependence of decomposition kinetics and product yields on pH and the lack of effect of N_3^- on the yield of **6a** and **8a** at neutral pH indicate that there are several competing pathways for the decomposition of **3a** over the pH range examined. At pH < pK_a' the uncatalyzed decomposition of neutral **3a** via k_o dominates the product distribution. The quinol **4a** is clearly generated through an oxenium ion pathway, but **6a** and **8a** cannot be generated by that same pathway. At pH > pK_a' the product distribution is dominated by the uncatalyzed decomposition of $\mathbf{3a}^-$ via k_-. Under these conditions the only reaction product detected by HPLC is the phenol **6a**. Because **6a** derived under basic pH conditions is demonstrably generated from $\mathbf{3a}^-$ and $\mathbf{3a}^-$ cannot account for the small but readily detectable yield of **6a** under acidic and neutral pH conditions, there must be two independent pathways leading to **6a**. A mechanistic scheme consistent with the experimental data is presented in Scheme 3.

The scheme proposes that the three major decomposition products are generated by four different pathways. Paths **I** through **III** are proposed to account for the products generated from **3a** via k_o, whereas path **IV** is proposed to account for the generation of **6a** from $\mathbf{3a}^-$ via k_-.

Since the quinol **4a** is the most abundant product at pH < pK_a', path **I** is a major pathway for the decomposition of **3a** under these conditions. This pathway was previously described.[17] Evidence for the existence of **1a** includes the results of azide trapping experiments on both **2a** and **3a** and the direct detection and characterization of **1a** after laser flash photolysis of **2a**.[17,22,23] The results shown in Figure 4 demonstrate that the generation of **6a** and **8a** cannot be attributed to **1a**.

The rearrangement product **8a** is reminiscent of similar rearrangement products generated during the decomposition of *N*-arylhydroxylamine derivatives in aqueous solution.[28,29] The insensitivity of the yield of **8a** toward $[N_3^-]$ could be used to support a mechanism involving a concerted 1,3-rearrangement accompanying O−N bond cleavage[30] or, alternatively, an ion-pair rearrangement proceeding through a very short-lived tight ion pair.[28,29,31] In aqueous solution free ion **1a** is a relatively stable cation (lifetime = 170 ns) with a high azide/solvent selectivity ratio, k_{az}/k_s, of 1.0×10^3 M^{-1}.[17,22] A systematic study of the effect of arylnitrenium ion stability on the involvement of ion pairs in the hydrolysis of the corresponding esters of *N*-arylhydroxylamines found that if the nitrenium ion is highly selective with k_{az}/k_s in the range of that observed for **1a**, the yield of the rearrangement product arising from the ion pair is typically very low (less than 5%).[29] This is due to the fact that the ion pair has a very short lifetime in water (ca. 10^{-11} to 10^{-10} s), and if the ion is selective, the ion pair does not react significantly before diffusional separation occurs.[29,32] In the current case, the yield of rearrangement product **5** is almost equal to that of quinol **4a**, and the cation **1a** is highly selective. In order for the rearrangement product **8a** to be generated through the ion

(26) Jencks, W. P. *Acc. Chem. Res.* **1980**, *13*, 161–169.
(27) Richard, J. P.; Jencks, W. P. *J. Am. Chem. Soc.* **1982**, *104*, 4689−4691; **1982**, *104*, 4691−4692; **1984**, *106*, 1383−1396.
(28) Fishbein, J. C.; McClelland, R. A. *J. Chem. Soc., Perkin Trans. 2* **1996**, 663–671.
(29) Novak, M.; Kahley, M. J.; Lin, J.; Kennedy, S. A.; James, T. G. *J. Org. Chem.* **1995**, *60*, 8294–8304.
(30) Oae, S.; Sakurai, T. *Tetrahedron* **1976**, *32*, 2289–2294.
(31) Gutschke, D.; Heesing, A. *Chem. Ber* **1973**, *106*, 2379–2394. Gessner, U.; Heesing, A.; Keller, L.; Homann, W. K. *Chem. Ber* **1982**, *115*, 2865–2871.
(32) Hand, E. S; Jencks, W. P. *J. Am. Chem. Soc.* **1975**, *97*, 6221–6230. Eigen, M. *Angew. Chem., Int. Ed. Engl.* **1964**, *3*, 1–19.

Downloaded by EXETER UNIV on October 17, 2009 | http://pubs.acs.org
Publication Date (Web): September 23, 2009 | doi: 10.1021/jo9014062

SCHEME 3. Proposed Mechanistic Pathway for the Decomposition of 3a

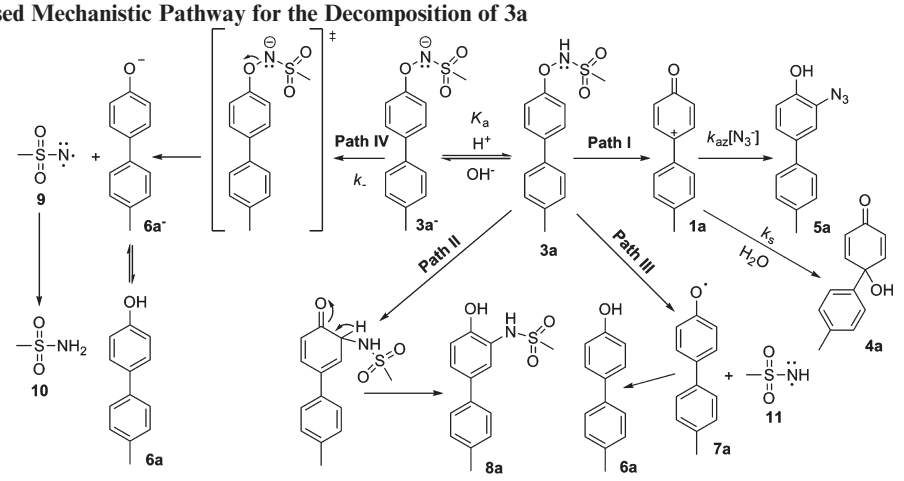

SCHEME 4. Possible Ion Pair Mediated Pathway

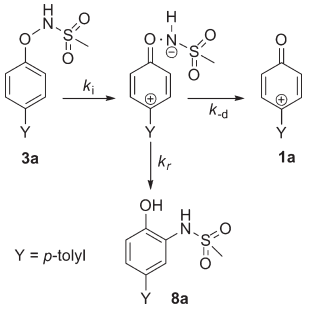

pair, k_r (Scheme 4) must be nearly equivalent to k_{-d}, the diffusion-limited rate constant for the ion-pair separation, based on the relative yields of **4a** and **8a** (ca. 1.1:1). However, a k_r of 10^{10} s^{-1} is ca. 100-fold larger than that observed in similar reactions of selective arylnitrenium ion pairs .[29] The anionic component of the ion pair in those cases was typically a carboxylate ion. The methylsulfonamide anion of the ion pair in Scheme 4 is expected to be a stronger nucleophile, so the ion-pair pathway cannot be ruled out.

The detection of a significant yield of **6a** (ca. 10%) at pH < pK_a' suggests that a third pathway for the reaction of **3a** (path **III**) occurs under acidic conditions. The triplet oxenium ion is an unlikely source of **6a** because recent calculations of the singlet−triplet gap for a variety of oxenium ions including **1a** indicate that the triplet state is about 20 kcal/mol less stable than the singlet state ion.[18,19] Also, if the triplet ion were in thermal equilibrium with the singlet ion **1a**, the yield of **6a** should be sensitive to [N_3^-]. The aryloxy radical **7a**, derived from a homolytic cleavage of the weak O−N bond, is a potential source of **6a**. It is known that **7a** derived from photolysis of **2a** in aqueous solution and CH_3CN gives rise to **6a**.[23] Photolysis results for **3a**, described below, also show that this substrate readily generates **7a** under conditions in which **2a** yields both **1a** and **7a**.

Under basic conditions the yield of phenol **6a** increases dramatically up to ca. 70−80%, whereas **4a** and **8a** are simultaneously suppressed and finally not detectable in NaOH solutions. The dominant form of **3a** in basic solution is the ionized species, **3a**$^-$; paths **I** and **II**, and **III** are no longer kinetically viable at pH > pK_a'. A stepwise base-catalyzed α-elimination (path **IV**) proceeding via **3a**$^-$ can explain the increasing generation of **6a** at pH > pK_a'. There can be little doubt that the rate-limiting step is the O−N bond dissociation, because **3a**$^-$ is detected spectrophotometrically at basic pH. This is consistent with the modest leaving group ability of **6a**$^-$.

This mechanism requires that the nitrene **9** is formed along with **6a**$^-$. Sulfonyl nitrenes, RSO_2N, are known reactive intermediates that can be generated from sulfonyl azides and other precursors by thermolysis in aprotic solvents or photolysis in protic solvents.[33,34] Methanesulfonyl nitrene, **9**, has a triplet ground state based on a triplet EPR signal observed at very low temperature.[35,36] Nitreme **9** can react as a diradical (triplet) undergoing H-abstraction or as an electrophile (singlet) inserting into aromatic or aliphatic hydrocarbons.[33,34] It was reported that **9**, generated from photolysis of methanesulfonyl azide in EtOH underwent both H-abstraction and O−H insertion leading to methanesulfonamide **10** (yield 43%) and *N*-ethoxymethanesulfonamide (yield 48%).[37] In an attempt to trap **9**, MeOH solutions containing 1 and 10 mM NaOMe were employed as reaction media for the decomposition of **3a** at 30 °C in the dark to replace the aqueous NaOH solutions. Authentic *N*-methoxymethanesulfonamide **12** was synthesized for comparison purposes.[38]

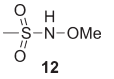

The reaction process was followed by HPLC and GC−MS. The decomposition rate of **3a** is dependent on [MeO^-]; **3a** decayed faster in MeOH solution with lower base concentration. Compared to the reaction of **3a** in basic aqueous solution, the decomposition in basic MeOH at the

(33) Abramovitch, R. A.; Sutherland, R. G. *Fortschr. Chem. Forsch.* **1970**, *16*, 1–33.
(34) L'abbé, G. *Chem. Rev.* **1969**, *69*, 345–363.
(35) Smolinsky, G.; Wasserman, E.; Yager, W. A. *J. Am. Chem. Soc.* **1962**, *84*, 3220–3221. Wasserman, E.; Smolinsky, G.; Yager, W. A. *J. Am. Chem. Soc.* **1964**, *86*, 3166–3167.
(36) Moriarty, R. M.; Rahman, M.; King, G. J. *J. Am. Chem. Soc.* **1966**, *88*, 842–843.
(37) Shingaki, T.; Inagaki, M.; Torimoto, N.; Takebayashi, M. *Chem. Lett.* **1972**, 1181–1184.
(38) Conway, T. T.; DeMaster, E. G.; Lee, M. J. C.; Nagasawa, H. T. *J. Med. Chem.* **1998**, *41*, 2903–2909.

Downloaded by EXETER UNIV on October 17, 2009 | http://pubs.acs.org
Publication Date (Web): September 23, 2009 | doi: 10.1021/jo9014062

Downloaded by EXETER UNIV on October 17, 2009 | http://pubs.acs.org
Publication Date (Web): September 23, 2009 | doi: 10.1021/jo9014062

same temperature was much slower. It required ca. 1 month for **3a** with an initial concentration of 0.01 M to disappear in 10 mM NaOMe/MeOH solution incubated at 30 °C. HPLC analysis of the reaction mixture shows that **6a** is the most significant decomposition product of **3a** in basic MeOH solution. The sulfonamide **10** was detected by GC−MS with an increasing yield during the course of the reaction. This is the expected product arising from triplet **9** through a H-abstraction mechanism. However, the expected O−H bond insertion product of singlet **9**, **12**, was not detected. This result is consistent with that recently reported by Desikan et al.[39] These workers reported a nearly quantitative yield of **10** for direct photolysis of a precursor of **9**, *N*-mesyl dibenzothiphene sulfilimine, in MeOH but no observation of **12**.[39] It is likely that in MeOH the singlet−triplet intersystem crossing is dominant over the reactions of singlet nitrene.

Photolysis Reactions. Previously we directly detected the generation of two transients, the cation **1a** and aryloxy radical **7a**, from nanosecond laser flash photolysis (ns-LFP) of quinol ester **2a** in aqueous solution and exclusive generation of **7a** from LFP of **2a** in CH_3CN.[22,23] Photolysis of **3a** was carried out at initial concentrations of ca. 1×10^{-5} M in N_2-saturated 5 vol % CH_3CN/H_2O buffered with pH 7.1 0.02 M phosphate buffer, and in N_2 or O_2-saturated CH_3CN with an initial concentration of **3a** of 5×10^{-5} M with UVC lamps. The aqueous reaction solutions were examined by HPLC immediately after short periods (15−45 s) of irradiation. Since the initial concentration of **3a** for the reactions in CH_3CN was higher and **3a** is unreactive in CH_3CN in the dark, photolysis of **3a** in CH_3CN was monitored by HPLC as the photolysis proceeded in short, punctuated (ca. 30 s) irradiation pulses for total irradiation times up to 360 s. HPLC analyses showed that there was little difference in photolysis products between the reactions in aqueous buffers and in CH_3CN, or between the reactions carried out in N_2-saturated and O_2-saturated reaction media. In all cases the phenol **6a** and the rearrangement product **8a** were formed as a result of photolysis. The initial relative yield of **6a** and **8a** is ca. 3:1 in aqueous solution and in CH_3CN. Both **6a** and **8a** decompose with long irradiation time but **8a** was more photosensitive than **6a**, so relative yields of the two photoproducts were determine after short UV pulses (ca. 15−30 s). Quinol **4a** was not identified as a photoproduct of **3a** in any experiment.

Compound **3a** was also subjected to ns-LFP (266 nm laser) in Ar- or O_2-saturated 50 vol % CH_3CN/H_2O buffered by pH 7.1 phosphate buffer, and in CH_3CN. The larger proportion of CH_3CN in the LFP experiments performed in the aqueous environment was necessitated by the need to increase the concentration of **3a** to obtain sufficient absorbance at 266 nm. The UV spectra for the reaction in O_2-saturated aqueous solution taken within 100 ns of the laser flash are shown in Figure 5. Two transient absorbance bands at λ_{max} 300 nm (A-300) and λ_{max} 360 nm (A-360) were observed. No significant absorbance band was observed at longer wavelength. An absorbance band at 360 nm that was attributed to the radical **7a** was previously observed during ns-LFP experiments on **2a**.[22,23] The band at 460 nm observed during the photolysis of **2a** that was attributed to the cation

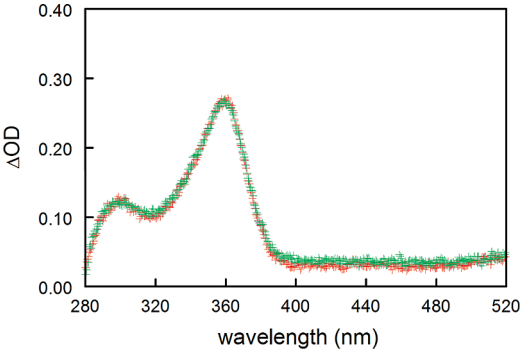

FIGURE 5. Transient absorbance spectra obtained after 266 nm excitation of **3a** in O_2-saturated 50 vol % CH_3CN/H_2O at pH 7.1. Key: red, 20 ns after the flash; green, 100 ns after the flash.

1a is not detected during photolysis of **3a** in an aqueous environment. The feature at 300 nm was not observed during photolysis of **2a**.[22,23] In CH_3CN the transient spectra are very similar except the 360 nm absorbance band has shifted to 350 nm. This same solvent-dependent shift was observed in the band attributed to **7a** during LFP experiments on **2a**.[22,23]

The bands decay over a period of ca. 500 μs. Kinetics of the decay of A-300 and A-360 monitored at 300 and 360 nm, respectively, at ambient temperature are summarized in Figure 6. The transient associated with A-360 decays in a biphasic manner. Data in Figure 6A were fit by a double exponential rate equation. Two rate constants derived from this fit are similar in the magnitude to those for the biphasic decay of **7a** previously observed in 5 vol % CH_3CN/H_2O (Table 4).[23]

On the basis of the evidence presented above, the transient species with λ_{max} 360 nm generated from LFP of **3a** is identified as aryloxy radical **7a**. Cation **1a** is not generated by photolysis of **3a** in aqueous solution. Its characteristic UV absorbance at 460 nm was not observed after LFP of **3a**. This indicates that the homolytic dissociation of **3a** to generate **7a** is the dominant process during the photolysis of **3a**. This conclusion is supported by the product study results of steady-state photolysis of **3a**: quinol **4a**, produced through the intermediacy of **1a**, was not observed under photolysis conditions. Instead, phenol **6a** was the most abundant photolysis product.

Modeling of the decay kinetics of the other transient species associated with A-300 is difficult because of the small absorbance change and the scattered data. Fitting the data by a triple exponential rate equation (Figure 6B) shows that an additional process with a large rate constant of $(3.22 \pm 0.46) \times 10^5$ s^{-1} occurs in the first few microseconds of the reaction. This rate constant is an order of magnitude larger than any of those observed for the decay of **7a**. The other two rate constants derived from the same fit, shown in Figure 6 appear to be comparable with the decay rate constants attributed to **7a** (Table 4). This indicates that the absorption at 300 nm is due, in part, to **7a** and to another shorter lived species. The absorbance band associated with **7a** that is generated during LFP of **2a** does have residual absorbance at 300 nm, so it is reasonable that the kinetics of decay of A-300 do include contributions from the decay of **7a**.[23] The identity of the short-lived species is unclear. It is not likely to be either singlet or triplet nitrene **9**, since **9** cannot be detected by ns-TRIR that has a lower detection limit of about 50 ns.[39]

(39) Desikan, V.; Liu, Y.; Toscano, J. P.; Jenks, W. S. *J. Org. Chem.* **2008**, *73*, 4398–4414.

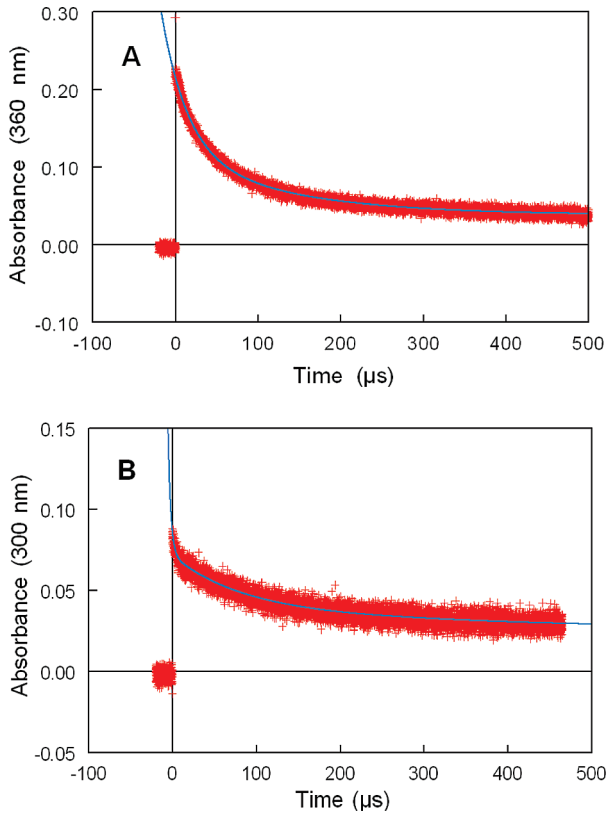

FIGURE 6. Decay of UV absorbance bands A-360 (A) and A-300 (B) in O_2-saturated pH 7.1 phosphate buffer (50 vol % CH_3CN/H_2O, μ = 0.5 ($NaClO_4$)). Data were fit to a double exponential rate equation (A) and a triple exponential equation (B) (blue curves).

TABLE 4. Decay Rate Constants for 7a in O_2-saturated 5 vol % CH_3CN/H_2O and for Two Absorbance Bands A-360 and A-300 Observed after LFP of 3a in O_2-Saturated 50 vol % CH_3CN/H_2O

transient/ conditions	k_1 (s^{-1})	k_2 (s^{-1})
decay of **7a** in 5 vol % CH_3CN/ H_2O, O_2 sat.[a]	$(8.06 \pm 0.08) \times 10^4$	$(1.29 \pm 0.02) \times 10^4$
decay of A-360 in 1/1 CH_3CN/ H_2O, O_2 sat.[b,d]	$(3.44 \pm 0.48) \times 10^4$	$(0.68 \pm 0.09) \times 10^4$
decay of A-300 in 1/1 CH_3CN/ H_2O, O_2 sat.[c,d]	$(1.45 \pm 0.13) \times 10^4$	$(0.24 \pm 0.23) \times 10^4$

[a]Data from ref 23. [b]Rate constants and error limits are averages and standard deviations of four independent measurements. [c]Derived from a single measurement. Three rate constants were obtained from the data fit; only the two smaller rate constants are shown. The larger rate constant is described in the text [d]All absorbance data except the data collected within the first 1 μs after the flash were used in data fitting.

Since the rearrangement product **8a** was also generated photochemically, this rapidly decaying species might be an intermediate leading to **8a**. Alternatively, it could be the radical **11**, the expected byproduct of the formation of **7a**. This species does not appear to have been described in the literature.

Conclusion

Originally methanesulfonylhydroxylamine **3a** was considered to be a potential precursor of the oxenium ion **1a**. Azide trapping that occurs without overall rate acceleration demonstrates that **3a**, similar to the quinol ester **2a**, does generate **1a** under solvolysis conditions. Unlike the hydrolysis of **2a**, however, ionization that leads to the cation **1a** is not the only pathway for the decomposition of **3a** in aqueous solution since three major products including the quinol **4a**, phenol **6a**, and rearrangement product **8a** were identified. The formation of these products is pH-dependent. The insensitivity of the yields of **6a** and **8a** to N_3^- indicates that they result from processes that do not involve **1a**. The rearrangement product **8a** is likely to be produced directly from **3a** through concerted intramolecular rearrangement or through rearrangement of an ion pair. Formation of phenol **6a** under acidic conditions may require homolysis of the O−N bond in **3a**. Formation of **6a** under basic conditions, on the other hand, occurs through a base-catalyzed α-elimination of **3a** via its conjugate base **3a**$^-$. The byproduct of the α-elimination is the nitrene **9**. Decomposition of **3a** in basic MeOH leads to formation of methanesulfonamide **10**, the expected product of H-abstraction by triplet nitrene **9**. The expected O−H insertion product, methoxymethanesulfonamide **12**, was not observed. This result is consistent with a recent observation that **9** generated photolytically in MeOH yields only **10**.[39]

It has been demonstrated that LFP of **2a** in aqueous solution generates two transient species, the oxenium ion **1a** and the aryloxy radical **7a**, that are responsible for the formation of a variety of photolysis products in aqueous solution. LFP of **3a** in aqueous solution does not generate **1a**, but the phenoxy radical **7a** is detected. These results are consistent with the observation that **6a** is a major photolysis product of **3a**, but **4a** is not detected in the photolysis reaction mixtures of **3a**. In addition to the biphasic decay of **7a** observed at 360 nm, another faster decay process is observed at 300 nm. Since both phenol **6a** and rearrangement product **8a** were generated from steady-state photolysis of **3a**, it is possible that the fast decay process observed at 300 nm is due to an intermediate leading to **8a**.

Although the quinol ester **2a** exclusively generates oxenium ion **1a** under hydrolysis conditions and is a reliable photoprecursor of **1a**, the generation of **1a** from the *O*-arylhydroxylamine derivative **3a** is less favorable. The oxenium ion pathway does account for a significant fraction of the reaction of **3a** under neutral and acidic conditions, but there are three other pathways that account for decomposition of **3a** under hydrolysis conditions. The phenol **6a** is generated by two different paths, one involving an apparent radical intermediate **7a** and the other proceeding via a stepwise α-elimination pathway through the conjugate base of **3a**, **3a**$^-$. The rearrangement product **8a** is also produced by a pathway that does not involve **1a**. Photolysis of **3a** does not generate **1a**. The weak O−N bond of **3a** is susceptible to homolysis under photolysis conditions, and the radical **7a** is readily observed after laser flash photolysis of **3a**. Photoinduced rearrangement to generate **8a** also is a minor pathway under photolysis conditions.

Because *O*-arylhydroxylamine derivatives have alternative reaction pathways and aromatic solvents are not effective at solvating cations, the previous attribution of oxenium ions as the source of the decomposition products of other *O*-arylhydroxylamine derivatives in aromatic solvents via thermolysis or acid-catalyzed decomposition (Scheme 1)

Downloaded by EXETER UNIV on October 17, 2009 | http://pubs.acs.org
Publication Date (Web): September 23, 2009 | doi: 10.1021/jo9014062

should be reconsidered. The previously observed phenol products[1−4,9] are likely generated by homolysis or α-elimination mechanisms. The predominance of *ortho*-substituted products[1−4,6−9] suggests an intramolecular pathway related to the process that generates **8a** in this study.

Experimental Section

Synthesis. The synthesis and characterization of **3a**, **4a**, and **6a** have been described previously.[17] The isolation and characterization of **8a** is described below. A sample of *N*-(methoxy)-methanesulfonamide **12** was obtained from a previously published procedure.[38]

Kinetic Studies. Kinetic studies of the decomposition reactions of **3a** were performed in 5 vol % CH_3CN/H_2O, μ = 0.5 ($NaClO_4$) over a wide range of pH at 30 °C in the dark. The pH was maintained with $HClO_4$ solutions (pH < 3.0), NaOH solutions (pH > 10.0), or with $HCO_2H/NaHCO_2$, AcOH/AcONa, NaH_2PO_4/Na_2HPO_4, $TrisH^+$/Tris base, and HCO_3^-/CO_3^{2-} buffers. Owing to the low solubility of **3a** in water, a 0.002 M stock solution of **3a** in CH_3CN was prepared and injected (15 μL) into 3 mL of reaction medium to obtain a low initial concentration of 1×10^{-5} M. Reactions were monitored by measuring the changes in UV absorbance as a function of time at all examined pH and by measuring the changes in the HPLC peak area as a function of time for **3a** and its decomposition products in pH 8.7, 9.2 Tris buffers, and pH 11.5 NaOH solution with dual wavelength monitoring. (HPLC condition: 20 μL injections on a 4.7 mm × 250 mm C-8 reverse phase column, 65/35 $MeOH/H_2O$ elution solvent, flow rate 1.0 mL/min). The wavelength chosen for monitoring the decomposition process varied slightly for different reaction media due to a slight shift of the maximum absorbance changes observed during a repetitive scan of the reaction solution: 227 and 260 nm used for reactions in all buffers, 232 and 269 nm for reactions in aqueous NaOH solutions. For the reactions monitored by UV spectroscopy, the observed rate constants were obtained as an average of two rate constants taken at each wavelength. For the reactions analyzed by HPLC, rate constants were obtained for each compound at the same wavelengths used for the UV study. The buffer effect on both reaction kinetics and product formation of **3a** was investigated in 0.01−0.04 M 1/9 NaH_2PO_4/Na_2HPO_4 buffers and in 0.01−0.04 M 3/1 $TrisH^+$/Tris base buffers, respectively. Control experiments were performed that measured the stability of rearranged product **8a** in pH 7.1 phosphate buffer and in pH 9.1 Tris buffer, and the stability of quinol **4a** in pH 12.8 NaOH solution at 30 °C. Reactions were initiated by injection of 15 μL of ca. 2 mM of stock solution of **4a** or **8a** in CH_3CN into 3 mL of the reaction solution incubated at 30 °C. The control mixtures were subjected to HPLC examination periodically. Most rate constants were evaluated by fits to a standard first-order rate equation. Formation and decay kinetics of **8a** in Tris buffer were determined by fitting the peak area versus time data to a double exponential rate equation.

Product Studies. The same reaction solutions of **3a** used for kinetic studies were subjected to HPLC analyses after the completion of the hydrolysis reaction. Individual yields of three major products were determined by HPLC quantification and studied as a function of pH over the pH range 4−13. HPLC conditions were 20 μL injections on a 4.7 mm × 250 mm C-8 reverse phase column, 65/35 $MeOH/H_2O$ elution solvent, flow rate 1.0 mL/min, monitoring wavelengths: 227, 260 nm for reactions in buffers, 232, 269 nm for reactions in NaOH solutions. Three major products were isolated from a large-scale hydrolysis reaction of **3a** in HOAc/NaOAc buffer at pH 4.6. A general procedure is as follows: **3a** (0.104 g, 0.376 mmol) was dissolved in 5 mL of CH_3CN, and the resulting solution was slowly added by syringe pump to 1 L of pH 4.6 0.02 M acetate buffer incubated at 40 °C. The steady-state concentration of **3a** in the reaction medium was maintained as ca. 1×10^{-5} M to avoid precipitation of **3a** during the reaction. After completion of the addition the mixture was incubated in the dark at 40 °C for another 10 half-lives (ca. 160 min; at 40 °C $t_{1/2}$ is ca. 16 min). The reaction was quenched by neutralization with saturated aqueous $NaHCO_3$ solution and was extracted with CH_2Cl_2 (3 × 250 mL) until HPLC examination indicated no products remained in the aqueous layer. The combined extract was dried over anhydrous Na_2SO_4, filtered, and evaporated to dryness under vacuum. The residue was subjected to separation and purification by multiple application of radial chromatography on silica gel using 20/1 CH_2Cl_2/EtOAc as eluent. Two products (**4a** and **6a**) are known compounds identified by comparison to authentic samples. The third product **8a** was characterized by NMR, IR, and LC-MS.

***N*-(4-Hydroxy-4′-methylbiphenyl-3-yl)methanesulfonamide (8a).** IR 3377, 3255, 3020, 2919, 1614, 1502, 1385, 1298, 1135, 1111, 983 cm^{-1}; ^1H NMR (300 MHz, DMSO-d_6) δ 2.32 (3H, s), 2.97 (3H, s), 6.96 (1H, d, J = 9.0 Hz), 7.23 (2H, d, J = 9.0 Hz), 7.33 (1H, dd, J = 10.4 Hz, 2.1 Hz), 7.44 (3H, m), 8.80 (1H, s(br)), 9.98 (1H, s(br)); ^{13}C NMR (75.5 MHz, DMSO-d_6) δ 20.6, 116.2, 124.3, 124.6, 124.7, 125.8, 129.4, 131.4, 135.8, 136.8, 150.3; LC-MS (ESI, positive) m/e 300 $(M + Na)^+$, 199 $(M - SO_2Me + H)^+$; (ESI, negative) m/e 276 $(M - H)^-$, 183 $(M - NHSO_2Me)^-$; high-resolution MS (ES, positive) $C_{14}H_{16}NO_3S$ (M + H) calcd 278.0845, found 278.0853; $C_{14}H_{15}NO_3SNa$ (M + Na) calcd 300.0664, found 300.0668.

Azide Trapping Studies. Azide trapping experiments were performed on the hydrolysis reaction of **3a** in pH 7.0, 0.02 M phosphate buffer (5 vol % CH_3CN/H_2O, μ = 0.5 ($NaClO_4$)) containing different amount of N_3^- (0.0005−0.03 M). HPLC examinations were performed on the reaction solutions after 10 half-lives (ca. 12 h). HPLC peak area for **6a** and **8a**, the decomposition products of **3a**, and for the azide adduct **5a** were plotted as a function of $[N_3^-]$. The production and characterization of azide adduct **5a** have been published elsewhere.[17] HPLC conditions were the same as those used for product studies but only the data obtained at 260 nm were used.

Attempted Trapping of Nitrene, 9. The decomposition of **3a** in 0.01 M MeONa/MeOH solution was monitored periodically by GC−MS and by HPLC until the HPLC peak for **3a** was no longer observable. **3a** (13.8 mg, 0.05 mmol) was directly added into 5 mL of basic MeOH solution incubated at 30 °C to gain an initial concentration of **3a** of 0.01 M. Simultaneously 0.01 M of **12** in the same basic MeOH solution was incubated at 30 °C as a control experiment. The samples used for HPLC analysis were prepared by diluting 100 μL of the reaction mixture with 1 mL of HPLC eluent. Another 100 μL of reaction mixture or the control experiment mixture was dried by a stream of N_2, redissolved in 50 μL of EtOAc, and then subjected to GC−MS examination. HPLC conditions were 20 μL injections on a 4.7 mm × 250 mm C-8 reverse phase column, 65/35 $MeOH/H_2O$ elution solvent, flow rate 1.0 mL/min, monitoring wavelengths: 227, 262 nm. GC−MS conditions were 30 m × 0.25 mm × 0.25 μm UF-35 ms column, initial column temperature 50 °C for 3 min, a 10 °C/min ramp to 250 °C, remaining at that temperature for 12 min, column pressure 0.1 psi. Identities of the major products generated from **3a** under this reaction condition were determined by comparison to the authentic samples using both HPLC and GC−MS.

Steady-State Photolysis Experiments. Steady-state photolyses of **3a** in 0.02 M pH 7.1 phosphate buffer (5 vol % CH_3CN/H_2O, μ = 0.5($NaClO_4$)) and in CH_3CN were performed in a Rayonet photochemical reactor in a jacketed quartz vessel kept at 30 °C. UVC lamps that have emission (ca. 90% of total lamp energy) in the range from 235 to 280 nm with a sharp maximum at 254 nm were used as the UV sources. A brief description of the

Downloaded by EXETER UNIV on October 17, 2009 | http://pubs.acs.org
Publication Date (Web): September 23, 2009 | doi: 10.1021/jo9014062

apparatus for steady-state photolysis has been published.[22] For reactions proceeding in the aqueous buffer, an initial concentration of ca. 1×10^{-5} M in **3a** was obtained by adding 0.5 mL of 0.002 M stock solution of **3a** in CH_3CN to 100 mL of N_2-saturated phosphate buffer. Reaction mixture was subjected to either 15 or 45 s irradiation. For reactions in CH_3CN, 5 mL of 0.01 M stock solution of **3a** in CH_3CN was injected into 100 mL of N_2- or O_2-saturated CH_3CN to obtain an initial concentration of **3a** of 5×10^{-5} M. Reactions performed in aqueous solutions were examined by HPLC immediately after the irradiation (C-8 reverse phase column, 65/35 MeOH/H_2O elution solvent, 1 mL/min, monitored by UV absorbance at 227 and 260 nm). In the reactions carried out in CH_3CN, **3a** was exposed to the UV irradiation for short intervals (ca. 30 s) for a total irradiation time of 270 s in N_2-saturated CH_3CN and 360 s in O_2-saturated CH_3CN. The reaction mixture was examined by HPLC after each irradiation in order to monitor the progress of the photoreaction.

Laser Flash Photolysis Experiments. A standard procedure provided elsewhere was employed for LFP of **3a**.[22,23] Laser flash photolysis was carried out using a Nd:YAG laser (266 nm, ~5 ns pulse) with 1 cm light path. All reactions were performed at ambient temperature (22 °C). Solutions of **3a** were made in O_2 or Ar saturated pH 7.1, 0.02 M phosphate buffer (50 vol % CH_3CN/H_2O, $\mu = 0.5(NaClO_4)$) by injecting 15 μL of ca. 0.02 M stock solution of **3a** into 3 mL of the buffer, so that the initial concentration of **3a** was ca. 2.5×10^{-4} M. Since **3a** undergoes slow hydrolysis under these conditions, all solutions were used promptly after mixing. Transient absorbance spectra were monitored in the range 280−540 nm. Kinetics of the decay of transients was monitored at 300 and 360 nm.

Acknowledgment. We thank the Donors of the American Chemical Society Petroleum Research Fund (Grant no. 43176-AC4) for support of this work. Y.-T.W. thanks the Department of Chemistry and Biochemistry at Miami University for a Dissertation Fellowship. The laser flash photolysis experiments were performed with the assistance of Jin Wang in the laboratory of Prof. Matthew S. Platz at The Ohio State University.

Supporting Information Available: Table S1, containing rate constants at various pH and buffer concentrations; Figure S1, showing the dependence of product yields on buffer concentrations; and ^1H and ^{13}C NMR spectra of **8a**. This material is available free of charge via the Internet at http://pubs.acs.org.

Downloaded by EXETER UNIV on October 17, 2009 | http://pubs.acs.org
Publication Date (Web): September 23, 2009 | doi: 10.1021/jo9014062